ISBN: 978-3-95450-232-5 ISSN: 2673-7000 doi:10.18429/JACoW-NAPAC2022-TUPA73

DESIGN AND LOW POWER TEST OF AN ELECTRON BUNCHING ENHANCER USING ELECTROSTATIC POTENTIAL DEPRESSION*

H. Xu†, B. E. Carlsten, Q. R. Marksteiner, Los Alamos National Laboratory, Los Alamos, NM, USA
B. L. Beaudoin, A. C. Ting, T. W. Koeth, University of Maryland, College Park, MD, USA

Abstract

We present our experimental design and low power test results of a structure for the proof-of-principle demonstration of fast increase of the first harmonic current content in a bunched electron beam, using the technique of electrostatic potential depression (EPD). A primarily bunched electron beam from an inductive output tube (IOT) at 710 MHz first enters an idler cavity, where the longitudinal slope of the beam energy distribution is reversed. The beam then transits through an EPD section implemented by a short beam pipe with a negative high voltage bias, inside which the rate of increase of the first harmonic current is significantly enhanced. An output cavity measures the harmonic current developed inside the beam downstream of the EPD section. Low power test results of the idler and the output cavities agree with the theoretical design.

INTRODUCTION

Non-relativistic bunched electron beams find uses in a variety of applications including microwave sources, such as traveling wave tubes and klystrons, and initial sections of a particle accelerator. A well bunched electron beam is marked by a high value of the first harmonic current. This paper addresses the design of an experiment for demonstrating a beam processing architecture, the electrostatic potential depression (EPD) [1], for enhancing the first harmonic current content in a bunched beam over a very short longitudinal distance.

A modulated beam with the bunching enhanced by the technique of EPD exhibits a higher first harmonic current compared to that produced by only a conventional idler cavity, and the high first harmonic current of the beam is maintained for a much longer beam travel distance after the EPD section, adding to the flexibility of the configuration of the beamline elements downstream.

An EPD element in the beamline is a section of the beam pipe with a negatively biased voltage U_{EPD} ($U_{\mathrm{EPD}} < 0$), as illustrated in Fig. 1. The beam pipe has an inner radius of r_w, and the solid electron beam has a radius of r_b. The Lorentz factors of the electron beam to be injected into the EPD section (γ_{inj}) and inside the EPD section (γ_0) have the relationship as given in Eq. (1),

$$\gamma_{\mathrm{inj}} = \gamma_0 - \frac{eU_{\mathrm{EPD}}}{m_e c^2} + \frac{I_0}{\beta_0 I_A}\left(1 + 2\ln\frac{r_w}{r_b} - \frac{r^2}{r_b^2}\right) \quad (1)$$

* Work supported by the U.S. Department of Energy Office of Science through the Accelerator Stewardship Program.
† haoranxu@lanl.gov

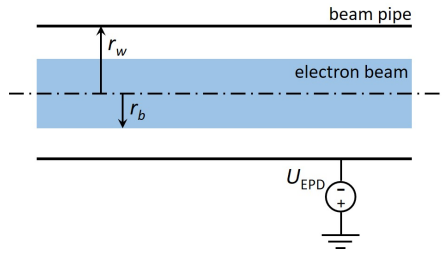

Figure 1: Configuration of an electrostatic potential depression (EPD) element.

where I_0 is the beam current, and $I_A = 4\pi\epsilon_0 m_e c^3/e = 17.0\,\mathrm{kA}$.

When a modulated electron beam enters the EPD section, the beam energy is reduced according to Eq. (1), but the energy modulation amplitude is preserved. According to the linear space charge wave theory [2], the wavelength of the space charge waves become smaller when the beam energy is reduced. As a result, at the space charge limit, the distance that the beam covers for the bunching development is shorter. Meanwhile, the nonlinear space charge wave theory [3] indicates that the electron bunching can be further enhanced if the depth of the energy modulation becomes substantially large compared to the average beam energy, which is scenario we are investigating inside the EPD section.

In addition, Eq. (1) indicates that in the case of a solid electron beam, for more consistent processing of the electron beam bunching by the EPD section exploiting the linear as well as nonlinear space charge effects, a beam with a smaller perveance is preferred.

EXPERIMENTAL SETUP

The planned experiment uses an inductive output tube (IOT) developed at the Naval Research Laboratory [4] as the bunched electron beam source.

The schematic of the experimental setup is shown in Fig. 2. The IOT electron gun operates at 710 MHz and produces 24-keV 0.55-A average current bunched beams, the first harmonic current of which monotonically decreases as the beam travels downstream. The oxygen-free high thermal conductivity (OFHC) copper idler cavity adjusts the longitudinal phase space of the bunches with a gap voltage of 6 kV so that the first harmonic current of the beam will start to increase, which is the identical scenario as in a generic klystron idler cavity. The EPD section is biased at −12 kV for the fast enhancement of the electron beam bunching. A stainless steel output cavity is used to extract the information of the harmonic current content in the beam, after which the

ISBN: 978-3-95450-232-5 ISSN: 2673-7000 doi:10.18429/JACoW-NAPAC2022-TUPA73

beam reaches the current monitor where the beam current is measured.

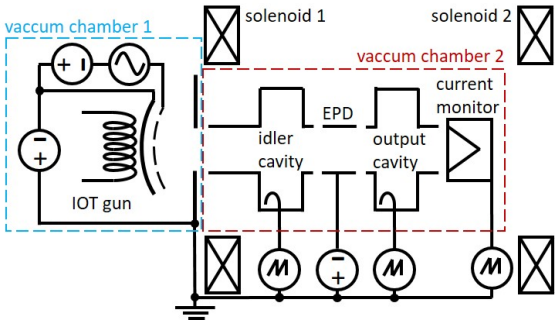

Figure 2: Schematic of the experimental setup using the IOT electron gun developed at the Naval Research Laboratory.

Semi-loop couplers with small coupling factor β are used on the sidewalls of the idler and the output cavities to detect the field strengths. The induced current of the first harmonic i_1 measures the first harmonic current in the bunched electron beam,

$$i_1 = (1+\beta)\frac{V_{\text{gap}}}{Z_{\text{cav}}} \tag{2}$$

and the gap voltage can be retrieved using the relationship in Eq. (3).

$$P_{\text{ext}} = \frac{|\beta|}{2}\frac{|V_{\text{gap}}|^2}{|Z_{\text{cav}}|} \tag{3}$$

The cavity coupler signals and the current monitor signal are measured by an oscilloscope.

SIMULATIONS

TUBE Simulations

The parameters including the gap positions and the gap voltages of the idler cavity and of the EPD section were determined by simulations using the 2.5D TUBE code, which allows for faster calculations compared to that by 3D particle-in-cell (PIC) codes. The input beam as from the IOT electron gun and the 2D gap field distributions for the TUBE simulations were generated beforehand using the CST simulation results.

The finalized positions and gap sizes of the idler cavity, EPD section, and the output cavity for the 710 MHz experiment are illustrated at the top of Fig. 3. The gap size of the idler and the output cavity is 10 mm, and that of the EPD gaps is 5 mm. The centers of the idler cavity, EPD decelerating gap, EPD re-accelerating gap, and the output cavity are located at 70 mm, 90 mm, 125 mm, and 160 mm downstream of the waist plane ($s = 0$) of the IOT gun.

The evolution of the average as well as the first harmonic current was also tracked in TUBE along the beam path. In Fig. 3, it can be seen that the the average current I_0 is constant, at 0.55 A. When there is only the 24 kV IOT gun in the simulation, the first harmonic current I_1 decreases monotonically (brown curve) due to the initial distribution of the electron bunch phase space formed at the gun. With

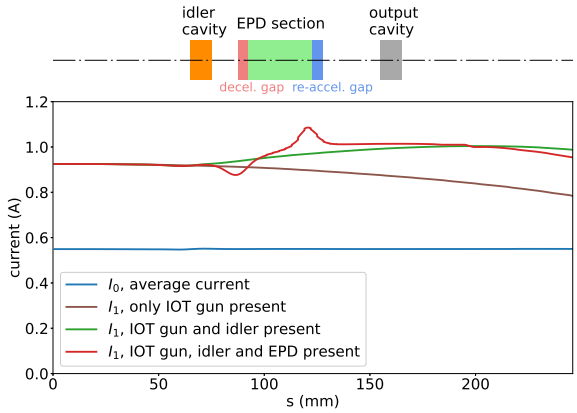

Figure 3: The TUBE results of the evolution of the first harmonic current along the propagation of the beam. The centers and the gaps of the idler cavity, EPD decelerating gap, EPD re-accelerating gap, and the output cavity are indicated in the diagram at the top of the plot.

the idler added in place with 6 kV gap voltage, the electron bunch longitudinal phase space distribution is modified and I_1 starts to increase (green curve), peaking at $s = 200$ mm, with $I_1 = 1.00\,\text{A} = 1.82 I_0$. After the −12 kV EPD section is added (red curve), the maximal value of I_1 reaches $I_1 = 1.01\,\text{A} = 1.84 I_0$, and the value of I_1 stays at 1.01 A from $s = 131$ to 195 mm.

With the EPD section implemented, the first harmonic current peak value is boosted, although slightly. In Fig. 3, the I_1 distribution shaped by the idler cavity alone has clear increase and decrease sections with a single peak value in between, however, with the addition of the EPD section, the high I_1 value is maintained as a plateau section downstream of the EPD, granting much more freedom to the positioning of the output cavity. Moreover, the EPD section brings the position of the maximal I_1 value closer to the upstream direction, shortening the total length of a potential structure.

CST Simulations

The entire structure was modeled and simulated in CST PIC solver for the confirmation of the field excitation inside the idler as well as the output cavity. The parameter setup used was identical to that in TUBE simulations. The gap voltage magnitudes in both cavities in the results from the CST simulation are given in Fig. 4.

CST PIC simulations were also performed without the output cavity, and the first harmonic current at the position of the output cavity center was calculated to be $I_1 = 1.89 I_0$. Then the EPD voltage was turned off, and this value decreased to $I_1 = 1.80 I_0$. This is in agreement with the TUBE results, attesting to the prediction that the EPD section moves the position of the increased I_1 further upstream.

Analytical estimate indicated that the idler cavity resonant frequency should be about 710.2 MHz to obtain the 6 kV gap voltage for an electron beam pre-bunched at 710 MHz. The cavity dimensions along with the tuner designs were determined by CST frequency domain simulations.

ISBN: 978-3-95450-232-5 ISSN: 2673-7000 doi:10.18429/JACoW-NAPAC2022-TUPA73

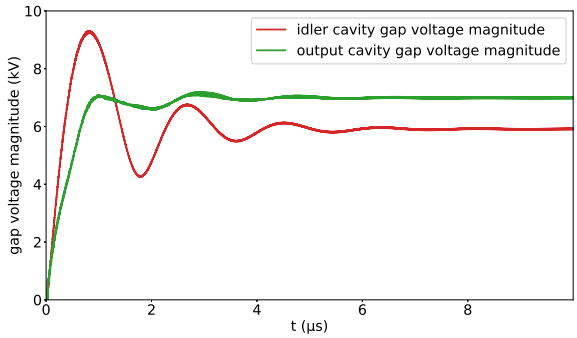

Figure 4: CST PIC simulation voltage probe results of the idler and the output cavities.

MECHANICAL FABRICATION

The vacuum chamber 2 (Fig. 2) and all the parts were fabricated at Jaguar Precision Machine, LLC. A sectional view of the assembled structure is shown in Fig. 5. A high voltage feedthrough is used to apply the negative high voltage to the EPD section, which is positioned in the bracket of Macor spacers, specially designed to avoid the concentration of the high direct current electric field at the triple point locations and to damp the parasitic modes.

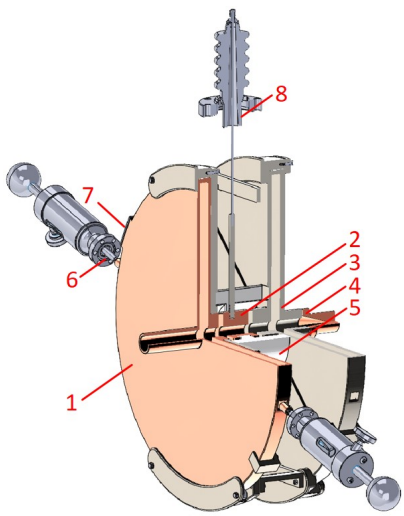

Figure 5: Assembly of the experimental structure. 1-idler cavity, 2-EPD section, 3-output cavity, 4-current monitor, 5-Macor spacers, 6-linear motion feedthrough for tuning, 7-semi-loop coupler port.

LOW POWER TEST

Low power tests were performed on the idler and output cavities, measuring the reflection coefficients (S_{11}). The results are shown in Fig. 6. The results shown were measured after the structure was assembled and the vacuum chamber was mounted to the output of the IOT electron gun. The idler cavity has a resonant frequency of $f_0 = 708.16$ MHz and an unloaded quality factor of $Q_0 = 2859$, and the output cavity has $f_0 = 708.01$ MHz and $Q_0 = 156$.

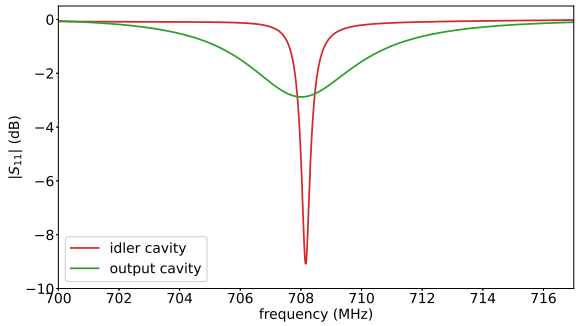

Figure 6: Reflection coefficient (S_{11}) measurement results of the idler and the output cavities.

The ratio of the cavity inner radius to the gap size is very large in the cavities, and there was deviation of the resonant frequencies of both cavities due to the deformation that took place in the assembly process. Additional mechanical tuning was performed to make corrections to the resonant frequencies.

CONCLUSION

We have designed and fabricated a structure for demonstrating the fast electron bunching enhancement by the technique of electrostatic potential depression (EPD). The low power tests of the cavities of the structure were performed and showed agreement with theoretical calculations. The beam test will be carried out using an inductive output tube (IOT) as the source of the pre-bunched electron beam.

Simulations in TUBE have predicted that an optimized EPD section as having been implemented in the experiment can increase the level of the first harmonic current achievable downstream, shift the axial position of the peak I_1 value upstream by a considerable amount, and give rise to a flat profile of the distribution of the enhanced I_1 downstream, adding to the design flexibility.

In the beam test, various experimental parameters will be attempted to verify the capability of the EPD technique in realizing fast enhancement of the first harmonic current of a bunched electron beam.

REFERENCES

[1] H. Xu *et al.*, "High efficiency compact microwave sources using electrostatic potential depression," *IEEE Trans. Electron Devices*, vol. 68, no. 4, pp. 1930–1935, 2021.

[2] R. J. Briggs, "Space-charge waves on a relativistic, unneutralized electron beam and collective ion acceleration," *Phys. Fluids*, vol. 19, no. 8, pp. 1257–1258, 1976.

[3] Y. Y. Lau *et al.*, "Nonlinear space-charge waves on an intense relativistic electron beam," *IEEE Trans. Plasma Sci.*, vol. 16, no. 2, pp. 249–257, 1988.

[4] S. H. Gold *et al.*, "Development of a high average current rf linac thermionic injector," *Phys. Rev. ST Accel. Beams*, vol. 16, no. 083401, 2013.